

# FINITE ELEMENT MODEL UPDATE VIA BAYESIAN ESTIMATION AND MINIMIZATION OF DYNAMIC RESIDUALS

Kenneth F. Alvin

*Structural Dynamics and Vibration Control Dept.*

*P.O. Box 5800*

*Sandia National Laboratories*

*Albuquerque, NM, 87185*

## *Abstract*

An algorithm is presented for updating finite element models based upon a minimization of dynamic residuals. The dynamic residual of interest is the force unbalance in the homogeneous form of the equations of motion arising from errors in the model's mass and stiffness when evaluated with the identified modal parameters. The present algorithm is a modification and extension of a previously-developed Sensitivity-Based Element-By-Element (SB-EBE) method for damage detection and finite element model updating. In the present algorithm, SB-EBE has been generalized to minimize a dynamic displacement residual quantity, which is shown to improve test-analysis mode correspondence. Furthermore, the algorithm has been modified to include Bayesian estimation concepts, and the underlying nonlinear optimization problem has been consistently linearized to improve the convergence properties. The resulting algorithm is demonstrated via numerical and experimental examples to be an efficient and robust method for both localizing model errors and estimating physical parameters.

## Nomenclature

|                       |  |
|-----------------------|--|
| $[M], [C], [K]$       | Nominal mass, damping and stiffness matrices   |
| $\omega_{Ei}$         | Experimental frequency (rad/s) for mode $i$  |
| $\{\phi_{Ei}\}$       | Experimental mode shape vector for mode $i$  |
| $\{R_i\}$             | Dynamic residual (modal force) vector  |
| $[Z_i]$               | Undamped impedance matrix for mode $i$   |
| $[ ]_m, [ ]_o$        | Measured, unmeasured partitions of $[ ]$   |
| $\Delta p$            | Change in parameter vector (i.e. $\Delta p = p^{(k)} - p^{(k-1)}$ at iteration $k$ ) |
| $[P_i]$               | Mode shape projection operator   |
| $[B_i]$               | Parameter sensitivities for mode $i$   |
| $J, \{g\}, [G]$       | Objective function, linearized gradient and Hessian                                  |
| $\delta\phi_{oi}$     | Variation of projected mode shape due to $\Delta p$                                  |
| $[Q_i]$               | Approximate covariance matrix of dynamic residual                                    |
| $[Q_{\phi_{mi}}]$     | Covariance matrix of measured mode shape   |
| $[Q_{\omega_i^2}]$    | Covariance matrix of the experimental eigenvalues                                    |
| $[Q_P]$               | Covariance matrix of the initial parameters  |
| $\overline{MAC}_{ij}$ | Mass-weighted modal assurance criteria   |

## I. Introduction

A significant amount of research in structural dynamics system identification has focused on methods for reconciling finite element models of structures with modal parameters identified from dynamic testing. Early approaches to this problem involved the direct updating of assembled stiffness and mass matrices to correlate to the available modes and mode shapes identified from test. In order to choose a particular solution from an infinite number of possible solutions, some quantity, such as the norm of the matrix adjustment, was minimized<sup>1,2</sup>. Recent modifications to this general approach involve retaining the connectivity pattern of the model through constraints<sup>3,4,5</sup>, or minimizing the rank of the matrix update<sup>6</sup>. These methods are efficient and have been used successfully for both model adjustments and for structural damage detec-

tion. When used in the context of model validation, the adjusted matrices are intended to guide the analyst in revising the finite element model's global and elemental parameters in a manner consistent with the specific design, the underlying physics, and the finite element method. For this discussion, this class of methods can be termed optimal matrix updating.

A fundamentally different approach involves estimating or updating the “physical” parameters of the structural design, such as cross-sectional areas, elastic moduli, or added masses, used in the finite element model definition<sup>7,8,9,10</sup>. There are a number of advantages to such an approach over optimal matrix updating methods. First, the formulation of the initial model, including its connectivity, is implicitly preserved. Secondly, results of model updating can be understood in terms of errors in design parameters or modeling assumptions. This provides a mechanism, at least ideally, for learning and improving the future modeling of similar structures. Finally, the updated model is directly useful for design sensitivity analysis as it retains the form of the finite element model data, without requiring additional interpretations such as is the case with the optimal matrix updating approach. It should be noted, however, that the generality and utility of the updated model depends critically on the selection of parameters to be adjusted, and thus the selection of parameters (i.e. model error localization) can itself introduce significant error. The approach of estimating model parameters is termed sensitivity-based model updating, as it utilizes the sensitivity of predicted and estimated quantities, such as modal parameters or response functions, to the physical parameters of the model.

The present paper addresses the problem of sensitivity-based model updating through the minimization of a dynamic residual. This residual arises due to errors in the model stiffness and mass matrices and is a reflection of the difference between the model's predicted modal parameters and the modal parameters from experimental data<sup>11</sup>. It is a different approach, however, from directly comparing the predicted and measured modal parameters and does not require the computation of the model modes and determination

of the correspondence between the model modes and the test modes. This is a distinct advantage, both in terms of computational expense and in reducing the complexity to the user, since such mode-to-mode correspondence can be difficult to establish when significant modeling errors exist. The present algorithm is a modification and extension of a previously-developed Sensitivity-Based Element-By-Element (SB-EBE) method for finite element model updating<sup>10</sup>. Hemez<sup>12</sup> provides a more detailed literature review and comparison of SB-EBE and other sensitivity-based algorithms for the interested reader.

The modifications of the basic SB-EBE algorithm address a number of practical issues encountered when applying the algorithm to complex structures. First, a consistent linearization of the governing minimization problem is derived to improve the rate of convergence of the algorithm. The new linearization couples the mode shape projection and parameter estimation stages of the algorithm at a minor computational cost, and improves the estimate of curvature in the optimization space. Secondly, the residual governing the update problem is redefined as a displacement, rather than force, quantity through a flexibility weighting. It is shown that this weighting improves the correspondence of test and analysis modal parameters typically used to assess the model's accuracy. Finally, Bayesian estimation<sup>13</sup> is incorporated to condition the update problem. Bayes estimation involves the use of relative confidence measures for the parameters being updated and the observed data used to guide the estimation. This important modification leads to a more reliable algorithm, especially in the presence of small sensitivity coefficients, large model errors, and correlation between parameters.

The remainder of the paper is organized as follows. In Section 2, the basic SB-EBE theory and algorithm is reviewed. In Section 3, the new modified algorithm is developed theoretically and its implementation is detailed in Section 4. Numerical and experimental results are given in Section 5, and Section 6 offers concluding remarks.

## II. Review of Basic Theory and Algorithm

The governing equations for linear time-invariant structural dynamics are typically given as

$$M\ddot{q} + C\dot{q} + Kq = \hat{B}u \quad (1)$$

where  $K$ ,  $C$ , and  $M$  are the stiffness, damping, and mass matrices from the finite element model,  $q$  is a vector of displacements,  $u$  is a vector of applied forces, and  $\hat{B}$  maps those forces to the associated degrees of freedom of the model. The homogeneous form of Eqn. (1) leads to the following undamped generalized eigenproblem:

$$K\phi = \lambda M\phi \quad (2)$$

where  $\lambda$  is the eigenvalue, which is equal to  $\omega_n^2$ , the square of the undamped natural frequency, and  $\phi$  is the associated eigenvector, which is physically the normal (i.e. undamped) mode shape.

The basic SB-EBE theory<sup>10</sup> determines the change  $\Delta p$  to a set of physical parameters of the model which minimize the norm of the dynamic force residual, viz.

$$\min_{\Delta p} \left( \sum_i \|R_i\|_2^2 \right) \quad (3)$$

$R_i$  is the dynamic force residual for mode  $i$ , defined as

$$R_i = (K - \omega_{E_i}^2 M)\phi_{E_i} \quad (4)$$

where  $\omega_{E_i}$  is an experimentally-determined normal frequency of the structure for mode  $i$ , and  $\phi_{E_i}$  is the associated normal mode shape. Unfortunately, the degrees of freedom (DOF) at which the mode shape is sampled from test is typically much smaller than the number of DOF in the finite element model which defines  $K$  and  $M$ . Therefore, to apply Eqn. (4), either the model must be reduced to the measurement DOF, or the measured portion of the mode shape must be expanded to the displacement basis of the model. The

original SB-EBE algorithm uses an expansion of the experimental mode shapes to compute the dynamic residual, which is advantageous because it provides an estimate of the dynamic residual in terms of the full displacement set of the model, facilitating error localization.

The theoretical basis for correcting the model using the dynamic force residual is as follows. If the “correct” model is given as

$$\begin{cases} K_c = K + \Delta K \\ M_c = M + \Delta M \end{cases} \quad (5)$$

and from Eqn. (2)

$$(K_c - \omega_{E_i}^2 M_c) \phi_{Ei} = 0 \quad (6)$$

then

$$-R_i = (\Delta K - \omega_{E_i}^2 \Delta M) \phi_{Ei} \quad (7)$$

Hence,  $R_i$  is a function of both magnitudes and spatial locations of the model errors. The basic Hemez algorithm consists of three key steps: mode shape projection, error localization (parameter selection), and parameter estimation. The algorithm is iterative; the mode shapes are projected using the current model (which is in error), and then the projected shapes are used in computing the parameter updates. The model mass and stiffness matrices are then updated at each iteration with the parameter variations and the next iteration begins. Thus as the iterations proceed, the model and hence the mode shape projections improve, leading to better parameter estimates and so on. The iterations conclude when the magnitude of the parameter variations fall below a user-defined threshold. The algorithm steps are detailed in the following subsections.

## A. Mode Shape Projection

To derive the proper projection operator from Eqn. (3), we must partition the mode shape  $\phi_i$  into its measured and unmeasured components, and also partition the associated columns of the mass and stiffness matrices. Then

$$\begin{aligned} R_i &= (K - \omega_{E_i}^2 M) \phi_{E_i} \\ &= \left( \begin{bmatrix} K_m & K_o \end{bmatrix} - \omega_{E_i}^2 \begin{bmatrix} M_m & M_o \end{bmatrix} \right) \begin{Bmatrix} \phi_{Em_i} \\ \phi_{o_i} \end{Bmatrix} \end{aligned} \quad (8)$$

where  $\phi_{Em_i}$  is the mode shape for mode  $i$  at the measurement DOF,  $\phi_o$  is the unmeasured portion of the same mode shape, and  $K_m$ ,  $M_m$ ,  $K_o$ , and  $M_o$  are the measured and unmeasured column sets of the stiffness and mass matrices. The mode shape projection directly results from minimizing the dynamic residual with respect to  $\phi_o$ , assuming no change in the model parameters, viz.

$$\min_{\phi_o} R_i^T R_i \quad (9)$$

Defining  $Z_i = K - \omega_{E_i}^2 M$  as the dynamic stiffness of mode  $i$  and partitioning  $Z_i$  into sets  $m$  and  $o$ , the residual  $R_i$  can be written as

$$R_i = \begin{bmatrix} Z_{m_i} & Z_{o_i} \end{bmatrix} \begin{Bmatrix} \phi_{Em_i} \\ \phi_{o_i} \end{Bmatrix} \quad (10)$$

Therefore, the minimization problem is

$$\min_{\phi_{o_i}} \phi_{Em_i}^T Z_{m_i}^T Z_{m_i} \phi_{Em_i} + 2 \phi_{o_i}^T Z_{o_i}^T Z_{m_i} \phi_{Em_i} + \phi_{o_i}^T Z_{o_i}^T Z_{o_i} \phi_{o_i} \quad (11)$$

which leads to the mode shape projection

$$\begin{aligned}
\phi_{o_i} &= -(Z_{o_i}^T Z_{o_i})^{-1} Z_{o_i}^T Z_{m_i} \phi_{Em_i} \\
&= P_{oi} \phi_{Em_i} \\
\therefore \phi_{E_i} &= \begin{Bmatrix} \phi_{Em_i} \\ \phi_{o_i} \end{Bmatrix} = \begin{bmatrix} I \\ P_{oi} \end{bmatrix} \phi_{Em_i} = P_i \phi_{Em_i}
\end{aligned} \tag{12}$$

After the projection operator  $P_i$  for mode  $i$  is determined, the mode shape is projected and the dynamic force residual  $R_i$  with respect to the model DOF can be computed. The force residual is then given by

$$\begin{aligned}
R_i &= Z_i \phi_{E_i} = \begin{bmatrix} Z_{mi} & Z_{oi} \end{bmatrix} \begin{bmatrix} I \\ -(Z_{oi}^T Z_{oi})^{-1} Z_{oi}^T Z_{mi} \end{bmatrix} \phi_{Em_i} \\
&= \left( I - Z_{oi}^T (Z_{oi}^T Z_{oi})^{-1} Z_{oi}^T \right) Z_{mi} \phi_{Em_i}
\end{aligned} \tag{13}$$

## B. Error Localization

Recalling Eqn. (7), the DOF exhibiting the largest force residuals will be associated with the set of model elements whose parameters are significantly in error. Therefore, it is reasonable to select those parameters which cause the largest perturbations to the element matrices associated with a set of model DOF  $j$ , where  $R(j)$  is above some threshold level. In the original SB-EBE method this process is termed “zooming.”

## C. Parameter Estimation

The final step, after projecting the mode shapes and choosing which model parameters to vary, is to compute the updated parameter values which minimize the sum of dynamic force residuals over a set of modes, viz.

$$\min_{\Delta p} \sum_i R_i^T R_i \tag{14}$$

The estimator is determined by expanding  $R_i$  in a first-order Taylor series with respect to the parameter variations  $\Delta p$ :

$$\begin{aligned} R_i + \delta R_i &= Z_i \phi_i + \sum_j \left( \frac{\partial Z_i}{\partial p_j} \phi_i \right) (\Delta p_j) \\ &= R_i + B_i \Delta p \end{aligned} \quad (15)$$

where

$$\begin{aligned} \frac{\partial Z_i}{\partial p_j} &= \frac{\partial K_i}{\partial p_j} - \omega_{E_i}^2 \frac{\partial M_i}{\partial p_j} \\ B_i &= \begin{bmatrix} B_{i1} & \dots & B_{ij} & \dots & B_{ip} \end{bmatrix} \quad B_{ij} = \frac{\partial Z_i}{\partial p_j} \phi_i \end{aligned} \quad (16)$$

and  $R_i$  is computed from Eqn. (8) using the projected mode shape  $\phi_{E_i}$  obtained from Eqn. (12). Here,  $B_i$  is the sensitivity of  $R_i$  to the parameters being updated. Plugging Eqn. (15) into Eqn. (14) and minimizing with respect to the parameter variations  $\Delta p$ , we have

$$G \Delta p = -g \quad (17)$$

where

$$G = \sum_i B_i^T B_i \quad g = \sum_i B_i^T R_i \quad (18)$$

and the update is given as

$$\begin{aligned} \Delta p &= -G^{-1} g \\ K &= K + \sum_j \frac{\partial K}{\partial p_j} (\Delta p_j) \\ M &= M + \sum_j \frac{\partial M}{\partial p_j} (\Delta p_j) \end{aligned} \quad (19)$$

### III. New Algorithm: Theory

The motivation for developing a new algorithm based upon the SB-EBE method came from tests of that algorithm on a moderately simple beam structure which will be reviewed in a later section. These tests revealed a number of problems, including small magnitude parameter updates leading to slow convergence, and convergence to poor solutions as measured by frequency errors and mode shape correlations.

Based on the above concerns, the basic theory and algorithm was re-worked to incorporate:

- Consistent linearization of the optimization problem
- Generalization of the modal error vector
- Inclusion of Bayesian estimation concepts to regularize the updating equations

We now proceed to detail these modifications.

#### A. Consistent linearization of the optimization problem

The solution proposed by the basic algorithm is staggered in the following sense. Although the model is being adjusted in the overall procedure, this adjustment is ignored in the determination of the mode shape projection. While this simplifies the theory somewhat, it may introduce a serious computational cost. By ignoring the coupling between the projection and the parameter estimation, the curvature of the parameter space is poorly estimated. The result is that the curvature is artificially large, leading to smaller parameter changes and much slower convergence.

This problem can be alleviated by adding a correction  $\delta\phi_{oi}$  to the projected partition of the mode shapes which accounts for the mode shape dependence on the parameter variation in a consistent manner.

Using

$$\begin{aligned}\phi_{oi} &= -(Z_{oi}^T Z_{oi})^{-1} Z_{oi}^T Z_{mi} \phi_{Emi} + \delta\phi_{oi} \\ &= P_{oi} \phi_{Emi} + \delta\phi_{oi}\end{aligned}\tag{20}$$

the residual  $R_i$  is given as

$$\begin{aligned}
R_i + \delta R_i &= \left( Z_i + \sum_j \left( \frac{\partial Z_i}{\partial p_j} \right) \Delta p_j \right) (\phi_i + \delta \phi_i) \\
&= R_i + B_i \Delta p + Z_{oi} \delta \phi_{oi} + \sum_j \left( \frac{\partial Z_{oi}}{\partial p_j} \delta \phi_{oi} \right) \Delta p_j
\end{aligned} \tag{21}$$

and the minimization problem (ignoring terms higher than second-order) is

$$\min_{\Delta p, \delta \phi_{oi}} J = \sum_i J_i \tag{22}$$

where

$$\begin{aligned}
J_i &= R_i^T R_i + 2 \Delta p^T B_i^T (R_i + Z_{oi} \delta \phi_{oi}) + 2 \delta \phi_{oi}^T Z_{oi}^T R_i + \Delta p^T (B_i^T B_i) \Delta p \\
&\quad + \delta \phi_{oi}^T Z_{oi}^T Z_{oi} \delta \phi_{oi} + 2 R_i^T \sum_j \left( \frac{\partial Z_{oi}}{\partial p_j} \delta \phi_{oi} \right) \Delta p_j
\end{aligned} \tag{23}$$

The first-order conditions are:

$$\begin{aligned}
\frac{\partial J}{\partial \Delta p_j} &= \left( \sum_i B_{ij}^T B_i \right) \Delta p + \sum_i \left( B_{ij}^T Z_{oi} + R_i^T \left( \frac{\partial Z_{oi}}{\partial \Delta p_j} \right) \right) \delta \phi_{oi} + \sum_i B_{ij}^T R_i = 0 \\
\frac{\partial J}{\partial \delta \phi_{oi}} &= (Z_{oi}^T Z_{oi}) \delta \phi_{oi} + \sum_j \left( Z_{oi}^T B_{ij} + \left( \frac{\partial Z_{oi}}{\partial \Delta p_j} \right)^T R_i \right) \Delta p_j = 0
\end{aligned} \tag{24}$$

since  $Z_{oi}^T R_i = Z_{oi}^T (I - Z_{oi} (Z_{oi}^T Z_{oi})^{-1} Z_{oi}^T) Z_{mi} \phi_{Emi} = 0$ .

Thus, the linearized coupled system of equations is given as:

$$\begin{bmatrix} \sum_i B_i^T B_i & c_1 & c_2 & \dots & c_N \\ c_1^T & Z_{o1}^T Z_{o1} & 0 & \dots & 0 \\ c_2^T & 0 & Z_{o2}^T Z_{o2} & \dots & 0 \\ \vdots & \vdots & \vdots & \ddots & \vdots \\ c_N^T & 0 & 0 & \dots & Z_{oN}^T Z_{oN} \end{bmatrix} \begin{bmatrix} \Delta p \\ \delta\phi_{o1} \\ \delta\phi_{o2} \\ \vdots \\ \delta\phi_{oN} \end{bmatrix} = \begin{bmatrix} -\sum_i B_i^T R_i \\ 0 \\ 0 \\ \vdots \\ 0 \end{bmatrix} \quad (25)$$

where

$$c_i^T = Z_{oi}^T B_i + \left[ \left( \frac{\partial Z_{oi}}{\partial \Delta p_1} \right)^T R_i \quad \left( \frac{\partial Z_{oi}}{\partial \Delta p_2} \right)^T R_i \quad \dots \quad \left( \frac{\partial Z_{oi}}{\partial \Delta p_{np}} \right)^T R_i \right] \quad (26)$$

Finally, noting the special form of Eqn. (25), the mode shape perturbations  $\delta\phi_{oi}$  can be eliminated to yield the new parameter estimator

$$\begin{aligned} \bar{G} \Delta p &= -g \\ \therefore \Delta p &= -\bar{G}^{-1} g \end{aligned} \quad (27)$$

where

$$\begin{aligned} \bar{G} &= \sum_i (B_i^T B_i) - \sum_i \left( c_i (Z_{oi}^T Z_{oi})^{-1} c_i^T \right) \\ &= G - \sum_i \left( c_i (Z_{oi}^T Z_{oi})^{-1} c_i^T \right) \end{aligned} \quad (28)$$

and  $G, g$  are given by Eqn. (18).

Comparing Eqn. (18) to Eqn. (28), it is seen that the consistent linearization changes the curvature of the design space  $\bar{G}$ , generally reducing its magnitude. This formulation introduces only a modest increase in computations as the factorization of  $Z_{oi}^T Z_{oi}$  is already computed during the mode shape projection step and thus can be saved for use in Eqn. (28). The introduction of this consistent linearization, however, dra-

matically improves the convergence of the algorithm, as will be shown in the numerical example problem.

## B. Generalization of the modal error vector

The objective function selected for the optimization problem, Eqn. (3), is by no means the only clear choice for performing finite element model update. Its advantage is that it does not require solving for the modes of the finite element model, and tracking those analytical modes with respect to the test modes. Its disadvantage, however, is that the updated model may not improve the errors between the analysis and test frequencies, or improve the correlation of the mode shapes. In fact, these accuracy indicators may be significantly degraded, and the resultant model cannot be judged as accurate as the initial model.

In seeking to understand the convergence of the basic algorithm to poor solutions as measured by errors in the updated frequencies and mode shapes, it is helpful to compare the dynamic residual to traditional modal parameter-based error metrics. First, we can re-write the contribution of mode  $i$  to the objective function in equivalent modal parameter terms, viz.

$$R_i^T R_i \approx \alpha_i \sum_j (\omega_j^2 - \omega_{Ei}^2)^2 (MAC_{ij}) \quad (29)$$

where  $j$  ranges over all possible modes of the finite element model, and

$$\overline{MAC}_{ij} = \frac{(\phi_j^T M \phi_{Ei})^2}{(\phi_j^T M \phi_j)((\phi_{Ei})^T M \phi_{Ei})} \quad \alpha_i = (\phi_{Ei})^T M \phi_{Ei} \quad (30)$$

Here  $\overline{MAC}_{ij}$  is a mass-weighted variant of the Modal Assurance Criterion<sup>14</sup>, which is a normalized measure of the correlation between two mode shapes, in this case model mode  $j$  and test mode  $i$ . The parameter  $\alpha_i$  is the modal mass of the test mode shape. From Eqn. (29), the contribution to the overall dynamic force residual from test mode  $i$  is equivalent to summing up the squares of the differences between test eigenvalue  $i$  and each of the eigenvalues of the model, which are scaled by the correlation between the

test model shape and the associated model mode shape. Thus, if small correlations exist between the test mode shape and any model mode shapes with vastly different frequencies, the product of  $(\omega_i^2 - \omega_{E_i}^2)^2$  (which is large) with a small correlation coefficient  $\overline{MAC}_{ij}$  can lead to a term which can dominate the error index being minimized. This has the undesirable effect of biasing the algorithm away from reconciling test and model modes which correspond more closely in both mode shape and frequency.

To alleviate this problem, we can replace the modal force error by a generalized modal error  $\bar{R}_i = WR_i$ , where

$$\bar{R}_i^T \bar{R}_i \approx \alpha_i \sum_j \left( \frac{\omega_j^2 - \omega_{E_i}^2}{\omega_j^2} \right)^2 (\overline{MAC}_{ij}) \quad (31)$$

This result can be obtained approximately by defining  $W$  as

$$W = K^{-1} \text{ or } M^{\frac{1}{2}} K^{-1} \quad (32)$$

which implies that the generalized modal error is a dynamic displacement residual quantity, rather than a dynamic force residual. In this way, the problem of large error terms resulting from small correlations between modes with large differences in frequency has been mitigated by normalizing the error index by  $\omega_j^2$ .

### C. Including Bayesian estimation concepts

Although the parameters being estimated usually evolve from some nonzero initial estimate, the basic algorithm places no relative confidence on these initial values with respect to the test data used for model adjustment. The quantitative result is that there is no penalty placed on the magnitude of the parameter change. Therefore, any final parameter value, no matter what magnitude or sign, is judged as superior to the original estimate as long as the sum of the dynamic force residuals have been reduced. In actuality, there are usually both hard constraints placed on the parameter values and some degree of confidence in

the initial parameter estimates. Furthermore, the test data used for model adjustment is often imperfect, and the confidence in the data varies depending on whether frequency or mode shape component estimates are being considered.

A popular approach in estimation theory to address the aforementioned concerns is the use of Bayesian estimation<sup>13</sup>. For linear structural dynamics applications such as the present model updating problem, Bayesian estimation reduces to a generalized least-squares problem<sup>7</sup>. We can modify the performance index of the basic algorithm as follows:

$$\min_{\Delta p, \phi_{oi}} J \quad (33)$$

where

$$J = \sum_{i=1}^N \bar{R}_i^T Q_i^{-1} \bar{R}_i + \Delta p^T Q_p^{-1} \Delta p \quad (34)$$

$$Q_i = \text{diag}(Z_i P_i Q_{\phi_{mi}} P_i^T Z_i + Q_{\omega_i^2} M P_i (\phi_{mi} \phi_{mi}^T) P_i^T M)$$

$Q_p$  is the covariance matrix of the initial parameters being estimated,  $Q_{\phi_{mi}}$  is the covariance matrix of the components of measured mode shape  $i$ ,  $Q_{\omega_i^2}$  is the variance of the square of the measured modal frequency, and  $P_i$  is the mode shape projection matrix. The covariance matrix  $Q_i$  represents the variances of each component of the dynamic residual vectors  $R_i$ . The covariance matrices for the data,  $Q_{\phi_{mi}}$  and  $Q_{\omega_i^2}$ , are ideally obtained from statistical analysis of the measured data, while the covariances for the parameters,  $Q_p$ , are usually assumed relative to the other covariance matrices and is intended to reflect the confidence in the initial parameters values relative to the confidence in the data used for revising the parameters. See Appendix A for an detailed description of how the covariances matrices were obtained in the experimental example problem of Section V.

The primary difficulty in introducing the Bayesian estimation concept, or equivalently a maximum

likelihood estimator, is that the error quantity being minimized is not directly a measured quantity, hence the covariance being introduced is not simply the variances of the test data. Instead, the dynamic residual is a nonlinear function of the data, the model matrices and the mode shape projection. The mode shape projection is itself a function of the model and based on the minimization of the overall functional. Although introducing statistical measures can, in general, increase the robustness of the algorithm, this approach leads to nonlinearities because the mode shape projection and modal error covariance estimates are coupled.

#### IV. New Algorithm: Implementation

In this section we review the step-by-step procedure for the new modified algorithm and discuss implementation issues. The procedure is given in Box 1 and represents one pass or iteration through the updating algorithm. Because of the inherent nonlinearity of the optimization, convergence to a solution can require many iterations. As noted previously, the mode shape projection and residual covariance computation given in Step 2b is actually a coupled problem, because the projection is dependent on the scaling provided by the covariance matrix, while the covariance matrix depends on the projection. In the present work, this nonlinearity is handled in a very cursory manner by computing an initial estimate of  $Q_i$  using only the measured component of the mode shapes. This initial estimate of  $Q_i$  is used to compute an estimate of the mode shape projection. The mode shape projection estimate is used to re-compute a better estimate of  $Q_i$ , which is then used to complete the algorithm. This predictor-correction approach to estimating  $Q_i$  seems to work adequately for the applications studied. Other possibilities might include using a completely different mode shape projection algorithm to compute  $Q_i$ .

##### A. Control of Curvature Estimate

As mentioned in the preceding sections, a consistent linearization of the optimization is employed in

### Box 1: Summary of the Present Algorithm

Step 1. Given  $K, M, p_o, Q_p \quad \left\{ \frac{\partial K}{\partial p_j}, \frac{\partial M}{\partial p_j}, j = 1, \dots, n_p \right\}$

$$\left\{ \omega_{E_i}, \phi_{mi}^E, Q_{\omega_i^2}, Q_{\phi_{mi}}, i = 1, \dots, N \right\} \quad J = 0, g = 0, \bar{G} = Q_p^{-1}$$

Step 2. For modes  $i=1$  to  $N$

Step 2a. Form  $Z_i = W(K - \omega_{E_i}^2 M)$  and partition into  $Z_i = \begin{bmatrix} Z_{mi} & Z_{oi} \end{bmatrix}$

Step 2b. Compute  $Q_i$  using Eqn. (34), factor  $Z_{oi}^T Q_i^{-1} Z_{oi}$  and solve the mode shape projection:

$$(Z_{oi}^T Q_i^{-1} Z_{oi}) P_{oi} = -Z_{oi}^T Q_i^{-1} Z_{mi}$$

$$\phi_{oi} = P_{oi} \phi_{mi}$$

Step 2c. Compute  $R_i = Z_i \phi_i$ , sensitivities  $B_i = \begin{bmatrix} b_{i1} & b_{i2} & \dots & b_{inp} \end{bmatrix}$  where  $b_{ij} = W \left( \frac{\partial K}{\partial p_j} - \omega_{E_i}^2 \frac{\partial M}{\partial p_j} \right) \phi_i$

Step 2d. Compute  $c_i = \begin{bmatrix} c_{i1} & c_{i2} & \dots & c_{inp} \end{bmatrix}$ , where  $c_{ij}^T = b_{ij}^T Q_i^{-1} Z_{oi} + R_i^T Q_i^{-1} W \left( \frac{\partial K_o}{\partial p_j} - \omega_{E_i}^2 \frac{\partial M_o}{\partial p_j} \right)$

Step 2e. Solve  $(Z_{oi}^T Q_i^{-1} Z_{oi}) d_i = c_i$

Step 2f. Sum:

$$\begin{cases} J = J + R_i^T Q_i^{-1} R_i \\ g = g + B_i^T Q_i^{-1} R_i \\ \bar{G} = \bar{G} + B_i^T Q_i^{-1} B_i - c_i^T d_i \end{cases}$$

Step 3. Solve  $\bar{G} \Delta p = -g$

Step 4. Update  $K = K + \sum_j \left( \frac{\partial K}{\partial p_j} \right) \Delta p_j \quad M = M + \sum_j \left( \frac{\partial M}{\partial p_j} \right) \Delta p_j \quad p = p_o + \Delta p$

the modified algorithm to improve its convergence properties. Caution must be exercised, however, as this linearization does not guarantee a positive-definite hessian. The present procedure offers two mechanisms for controlling the curvature to avoid this result. The first is the use of Bayes estimation, which conditions the estimation problem by contributing a penalty term on the change in the parameter estimates. Numerically, this term provides a positive-definite contribution to the hessian which can be adjusted to reflect the analyst's relative confidence in the initial parameter estimates.

The second mechanism for controlling the curvature estimate is through the use of a constant  $\beta$  which parameterizes the linearization between that of the basic algorithm ( $\beta = 0$ ) and the modified algorithm ( $\beta = 1$ ). This parameterization is utilized during the computation of  $\bar{G}$  in Step 6 of the procedure as

$$\bar{G} = \bar{G} + B_i^T Q_i^{-1} B_i - \beta(c_i^T d_i) \quad (35)$$

This constant controls the degree of coupling between the mode shape projection and the parameter estimation. Note that the basic algorithm is always guaranteed positive-definite, but that guarantee comes at the cost of a poorer estimate of the curvature. The use of the parameter  $\beta$  allows that cost to be controlled by the user.

## B. Model Reduction

Rather than projecting the mode shapes, reduction of the model to the measurement degrees of freedom can be employed<sup>15</sup>. This is often avoided because the static reduction of a refined model down to the small number of DOF measured will introduce errors in the predictive accuracy of the model, leading to nonzero dynamic residuals and inappropriate parameter corrections. A compromise is to employ a component mode synthesis type of reduction such as the Hurty/Craig-Bampton technique<sup>16,17</sup>, which augments a static condensation to the measurement DOF with a set of generalized DOF spanning the lowest eigenmodes of the omitted dynamics. Typically, the addition of a small number of generalized DOF is sufficient

to ensure that the reduced model can predict the lower eigenmodes of the full-order system. The intent is to guarantee that the differences between the experimental modes and the modes of the reduced model are primarily a function of the parameters of the full model and are not strongly influenced by the model reduction itself. The experimental modes would then be projected into this slightly larger subspace.

### C. Statistical Significance of the Parameter Estimates

An advantage of Bayes estimation is that it allows the analyst to assess the confidence intervals for the final estimates of the parameters, as a function of their initial covariances, their sensitivity to the experimental modal parameters used in the estimation, and the covariances of those parameters<sup>7</sup>. A linearized estimate of the covariance of the updated parameters is given by

$$\hat{Q}_p = G^{-1} = \left[ Q_p^{-1} + \sum \left\{ B_i^T Q_i^{-1} B_i - c_i (Z_{oi}^T Q_i^{-1} Z_{oi})^{-1} c_i^T \right\} \right]^{-1} \quad (36)$$

evaluated at the point of convergence. From this result, the standard deviation of the parameters can be determined by taking the square root of the diagonal elements of  $\hat{Q}_p$ . This statistical quantity is only as valid as the covariances of the experimental data and the initial parameters. The updated variances relative to their initial values are useful in determining whether the change in parameters is significant and based on the measured data.

## V. Applications

### A. Numerical Data: Planar Truss Structure

The first example from Reference 10 was chosen to test the implementation of the modified algorithm and assess its performance relative to the basic SB-EBE procedure. This example considers a free-free planar truss with 44 translational DOF, 7 of which are measured. For this comparison, the first 5 flexible

modes are used to update the model, and the only parameters being updated are the elastic modulus of two of the elements. Furthermore, the test data is assumed to be perfect (zero variance), which implies that the Bayesian covariance weights are not used. Thus the only differences between the two algorithms are the consistent linearization of the optimization problem and the weighting of the modal force error.

The results are documented in Table 1. Note that, although the use of the flexibility weighting does help to speed the convergence, it also introduces a computational overhead, especially when the weighting matrix is full rather than sparse. Note also that updating the weighting matrix at each iteration as the stiffness was updated did not improve the convergence of the algorithm. The need for weighting the modal error vector is dictated more by the quality of the final solution when the data is imperfect than by the convergence of the algorithm. Finally, it was found that using the full extent of the consistent linearization led to a negative curvature which caused the algorithm to diverge. Therefore,  $\beta$  was reduced to 0.95, which results in the fastest convergence. The CPU times given are for simple Matlab<sup>21</sup> implementation of the algorithms running under Matlab Vers. 4.2c on a HP700 workstation. The numbers shown are the mean of the estimated times from 30 identical analyses as computed using the `cputime` function in Matlab.

**Table 1: Comparison of Convergence Using Modified Algorithm**

| Method                  | Weighting Matrix                           | # update iterations | CPU time (sec) |
|-------------------------|--|---------------------|----------------|
| Basic SB-EBE            | N/A  | 180                 | 12.24          |
| Modified $\beta = 0.95$ | $W=I$<br>(modal force error minimization)  | 25                  | 2.30           |
| Modified $\beta = 0.95$ | $W = K_o^+$<br>(held constant)             | 8                   | 2.44           |
| Modified $\beta = 0.95$ | $W = K_{up}^+$<br>(updated each iteration) | 9                   | 3.55           |

The cases documented above were based upon the same convergence criterion. The parameter results

for the basic SB-EBE algorithm and the modified algorithm with  $W=I$  are shown in Figure 1. Note here that, even at 180 update iterations, the basic algorithm has still not reached the correct updated parameter values, while the modified algorithm with its consistent linearization has converged to within 1% of the correct values in less than 30 iterations

## **B. Experimental Data: LADDER Structure**

The experimental example problem is a tubular welded frame composed of thin-wall, rectangular steel tubing formed into a symmetric two rung ladder and representative of an automotive engine support. The test setup is shown in Figure 2. The structure was instrumented with 96 accelerometers grouped in 16 locations in order to extract both translational and rotational response at beam cross-sections throughout the structure. Excitation was effected through the use of an impact hammer and frequency response function (FRF) data were obtained using standard data reduction techniques. A modal model was then obtained using Polyreference<sup>18</sup> as implemented in SDRC's TDAS software package.

The finite element model of the structure is shown in Figure 3; it is a NASTRAN model consisting of CBEAM elements, with spring elements introduced to model the joint compliances. A detailed illustration of the modeling of the welded joint is shown in Figure 4. The goal of the model updating was primarily to determine the unknown joint compliance parameters, and to adjust the basic properties, in order to correlate the first 14 modes identified from test. A description of the nine design parameters considered in the updating analysis is given in Table 2. GRID locations were established to coincide with the physical locations of the accelerometers and these GRIDs were attached to the beams via multi-point constraints. The use of CBEAM elements was dictated by the need to correctly model the torsional inertia of the cross-section. The accelerometer masses were also incorporated into the model. The correlation of the modal parameters between the test-identified modes and the initial analysis model is documented in Table 3.

After attempts to reconcile the model using the basic SB-EBE procedure failed, the modified algorithm

**Table 2: Description of Modeling Parameters for Update**

| Parameter      | Description (x,y,z refer to Figure 4)               | Initial Value           |
|----------------|---|-------------------------|
| $K_{ux}$       | Localized joint spring in x-translational direction | 6.01e+6 N/mm            |
| $K_{uy}$       | Localized joint spring in y-translational direction | 6.01e+6 N/mm            |
| $K_{uz}$       | Localized joint spring in z-translational direction | 6.01e+6 N/mm            |
| $K_{\theta x}$ | Localized rotational joint spring about x-axis      | 2.53e+8 N-mm            |
| $K_{\theta y}$ | Localized rotational joint spring about y-axis      | 1.96e+8 N-mm            |
| $K_{\theta z}$ | Localized rotational joint spring about z-axis      | 4.80e+8 N-mm            |
| $I_1$          | Area moment of inertia about weak axis of tube      | 3.11e+5 mm <sup>4</sup> |
| $I_2$          | Area moment of inertia about strong axis of tube    | 5.89e+5 mm <sup>4</sup> |
| $J$            | Torsional constant of tube                          | 6.15e+5 mm <sup>4</sup> |

**Table 3: Initial LADDER Model/Test Comparison**

| Test Mode | Test Frequency (Hz) | Model Mode | Model Frequency (Hz) | %difference Frequency | Modal Assurance Criteria |
|-----------|---------------------|------------|----------------------|-----------------------|--------------------------|
| 1         | 78.9674             | 1          | 72.3633              | -8.36                 | 0.9973                   |
| 2         | 170.6259            | 3          | 174.9456             | 2.53                  | 0.9963                   |
| 3         | 174.4670            | 2          | 161.5404             | -7.41                 | 0.9934                   |
| 4         | 214.7231            | 4          | 206.3898             | -3.88                 | 0.9981                   |
| 5         | 250.9062            | 5          | 255.1062             | 1.67                  | 0.9951                   |
| 6         | 312.1717            | 7          | 318.6140             | 2.06                  | 0.9580                   |
| 7         | 315.7890            | 6          | 312.8396             | -0.93                 | 0.9516                   |
| 8         | 317.7661            | 9          | 368.6281             | 16.01                 | 0.9486                   |
| 9         | 330.2652            | 8          | 333.6956             | 1.04                  | 0.9968                   |
| 10        | 432.5194            | 10         | 451.6765             | 4.43                  | 0.9937                   |
| 11        | 518.5953            | 11         | 534.4661             | 3.06                  | 0.9890                   |
| 12        | 563.6540            | 14         | 806.4039             | 43.07                 | 0.8115                   |
| 13        | 612.8141            | 12         | 631.6433             | 3.07                  | 0.9816                   |
| 14        | 674.3648            | 13         | 678.9766             | 0.68                  | 0.7993                   |

was developed and applied to this problem. Initially, it was found that the joint spring parameters  $K_{ux}$  and  $K_{uz}$  had insufficient sensitivity to the measured modal parameters to be effectively estimated. Therefore,

those parameters were fixed for the duration of the updating procedure at their initial values, given in Table 2. The update evolved as follows: the joint rotational spring parameters were estimated based on the first 8 flexible modes with the model statically reduced to the 96 sensor DOF. This implies that no mode shape projection was performed. Then, cross-sectional parameters  $I_1$ ,  $I_2$  and  $J$ , which are the area moments of inertia and torsional constant of the beam elements, respectively, were added and estimated along with joint rotational springs using test modes 1-9 with the model statically reduced to the sensor DOF. The final values were estimated based on modes 1-12 with the same parameters plus  $K_{uy}$  and using the model reduced to measured DOF plus torsional DOF for model grids. This final estimation thus required that the mode shapes be projected. The procedures used to determine the covariance matrices for the analysis are described in Appendix A.

The resultant parameter values are given in Table 4. The correlation of the updated model to test for

**Table 4: Parameter Update Results for LADDER Structure**

| Parameter      | Final Value<br>(relative to initial) | Initial COV | Updated COV |
|----------------|--------------------------------------|-------------|-------------|
| $K_{uy}$       | 0.4250                               | 100%        | 0.49%       |
| $K_{\theta x}$ | 0.2580                               | 100%        | 0.00153%    |
| $K_{\theta y}$ | 104.0                                | 100%        | 3.58%       |
| $K_{\theta z}$ | 1.4621                               | 100%        | 1.39%       |
| $I_1$          | 0.9415                               | 3%          | 0.00663%    |
| $I_2$          | 0.9178                               | 3%          | 0.0191%     |
| $J$            | 1.0091                               | 3%          | 0.00661%    |

the first 14 modes are documented in Table 5. Observe that the frequency errors have been reduced from a maximum of 43% to below 4%, while the mode shape correlations have been maintained or slightly improved. Note also from the parameter update results that the updated coefficients of variation (COV),

**Table 5: Final LADDER Model/Test Comparison**

| Test Mode | Test Frequency (Hz) | Model Mode | Model Frequency (Hz) | %difference Frequency | Modal Assurance Criteria |
|-----------|---------------------|------------|----------------------|-----------------------|--------------------------|
| 1         | 78.9674             | 1          | 78.8034              | -0.21                 | 0.9978                   |
| 2         | 170.6259            | 2          | 169.6736             | -0.56                 | 0.9963                   |
| 3         | 174.4670            | 3          | 174.6665             | 0.11                  | 0.9931                   |
| 4         | 214.7231            | 4          | 218.2671             | 1.65                  | 0.9984                   |
| 5         | 250.9062            | 5          | 249.0289             | -0.75                 | 0.9957                   |
| 6         | 312.1717            | 6          | 307.9859             | -1.34                 | 0.9894                   |
| 7         | 315.7890            | 7          | 315.5987             | -0.06                 | 0.9789                   |
| 8         | 317.7661            | 8          | 323.0028             | 1.65                  | 0.8792                   |
| 9         | 330.2652            | 9          | 324.1070             | -1.86                 | 0.9521                   |
| 10        | 432.5194            | 10         | 435.3196             | 0.65                  | 0.9955                   |
| 11        | 518.5953            | 11         | 514.9591             | -0.70                 | 0.9894                   |
| 12        | 563.6540            | 12         | 542.8199             | -3.67                 | 0.8724                   |
| 13        | 612.8141            | 13         | 615.0687             | 0.37                  | 0.9732                   |
| 14        | 674.3648            | 14         | 673.2796             | -0.16                 | 0.8250                   |

which is the standard deviation of the parameter expressed as a percentage of the parameter value, is significantly smaller than the assumed initial COV. This implies that the parameters were highly sensitive to the modal data used in the estimation. Of course, the updated COV are directly a function of the assumed initial COV and the assumed variances of the experimental data, and so can only be considered relative to those assumptions. In conclusion, the present modified algorithm performed very well using the experimental data, resulting in a highly accurate updated model. One verification of the model accuracy is the improvement in the correlation of modes 13 and 14, whose errors were not used in the updating process.

## VI. Concluding Remarks

An algorithm for updating finite element models using modal data has been presented. The algorithm minimizes a generalized dynamic residual which is a function of the experimental modal parameters and

the model mass and stiffness matrices. The present algorithm is a modification of a previous method for sensitivity-based element-by-element model updating and incorporates a generalized error weighting, consistent linearization and Bayesian estimation. The algorithm has been demonstrated on numerical and experimental data and has been shown to be an efficient and effective approach for estimating parameters to reconcile test and analysis models.

### **Acknowledgments**

This work was supported by the United States Department of Energy under contract DE-AC04-94AL85000. Sandia is a multiprogram laboratory operated by Sandia Corporation, a Lockheed Martin Company, for the United States Department of Energy. The author wishes to thank Drs. John Red-Horse, Tom Carne, and Dave Martinez of Sandia Labs, Prof. Francois Hemez of Ecole Centrale Paris, and Prof. Charbel Farhat of the University of Colorado, Boulder for their help and encouragement.

### **REFERENCES**

1. Baruch, M., "Optimal Correction of Mass and Stiffness Matrices Using Measured Modes," *AIAA Journal*, Vol. 20, No. 11, 1982, pp. 1623-1626.
2. Berman, A. and Nagy, E. J., "Improvement of Large Analytical Model Using Test Data," *AIAA Journal*, Vol. 21, No. 8, 1983, pp. 1168-1173.
3. Kabe, A. M., "Stiffness Matrix Adjustment Using Mode Data," *AIAA Journal*, Vol. 23, No. 9, 1985, pp. 1431-1436.
4. Kammer, D. C., "Optimal Approximation for Residual Stiffness in Linear System Identification," *AIAA Journal*, Vol. 26, No. 1, 1988, pp. 104-112.
5. Smith, S. W. and Beattie, C. A., "Secant-Method Adjustment for Structural Models," *AIAA Journal*,

Vol. 29, No. 1, 1991, pp. 119-126.

6. Kaouk, M. and Zimmerman, D. C., "Structural Damage Assessment Using a Generalized Minimum Rank Perturbation Theory," *AIAA Journal*, Vol. 32, No. 4, 1994, pp. 836-842.
7. Collins, J. D., Hart, G. C., Hasselman, T. K., and Kennedy, B., "Statistical Identification of Structures," *AIAA Journal*, Vol. 12, No. 2, 1974, pp. 185-190.
8. Chen, J. C. and Garba, J. A., "Analytical Model Improvement Using Modal Test Results," *AIAA Journal*, Vol. 18, No. 6, 1980, pp. 684-690.
9. Hart, G. C. and Martinez, D. R., "Improving Analytical Dynamic Models Using Frequency Response Data - Application", *Proceedings of the 1982 AIAA Structures, Structural Dynamics and Materials Conference*, AIAA Paper 82-0637-CP, 1982.
10. Farhat, C. and Hemez, F. M., "Updating Finite Element Dynamic Models Using an Element-by-Element Sensitivity Methodology," *AIAA Journal*, Vol. 31, No. 9, 1993, pp. 1702-1711.
11. Ojalvo, I. U. and Pilon, D., "Diagnostics for Geometrically Locating Structural Math Model Errors from Modal Test Data, *Proceedings of 29th AIAA Structures, Structural Dynamics and Materials Conference*, AIAA Paper 88-2358-CP, Williamsburg, VA, 1988, pp. 1174-1186.
12. Hemez, F. M., "Theoretical and Experimental Correlation Between Finite Element Models and Modal Tests in the Context of Large Flexible Space Structure," Report CU-CSSC-93-18, Center for Aerospace Structures, University of Colorado, Boulder, CO, 1993, pp. 11-18.
13. Jazwinski, A. H., *Stochastic Processes and Filtering Theory*, Academic Press, San Francisco, 1970, pp. 145-158.
14. Ewins, D. J., *Modal Testing: Theory and Practice*, Research Studies Press Ltd., Somerset, England,

UK, 1984, pp. 225-226.

15. Guyan, R. J., "Reduction of Stiffness and Mass Matrices," *AIAA Journal*, Vol. 3, No. 2, 1965, p. 380.
16. Hurty, W. C., "Dynamic Analysis of Structural Systems Using Component Modes," *AIAA Journal*, Vol. 3, 1965, pp. 678-685.
17. Craig, R. R. and Bampton, M. C., "Coupling of Substructures for Dynamic Analyses," *AIAA Journal*, Vol. 6, No. 7, 1968, pp. 1313-1319.
18. Vold, H., and Rocklin, G. F., "The numerical implementation of a multi-input modal estimation method for mini-computers," *Proceedings of the 1st International Modal Analysis Conference*, SEM, Bethel, NY, 1983, pp. 542- 548.
19. Peterson, L. D. and Alvin, K. F., "A Time and Frequency Domain Procedure for Identification of Structural Dynamic Models," *Proceedings of the 36th Structures, Structural Dynamics and Materials Conference*, AIAA, Washington, DC, 1994.
20. Alvin, K. F., "Robust Model Error Localization For Damage Detection And Finite Element Model Update," *Proceedings of the Sixth International Conference on Adaptive Structures*, Key West, FL, 1995, pp. 305-315.
21. *MATLAB User's Guide*, The Mathworks Co., 1993.

## Appendix A: Determination of Covariance Matrices for Experimental Example Problem

The covariance matrices of the experimental parameters,  $Q_{\phi_{mi}}$  and  $Q_{\omega^2}$  were not directly available from statistical analysis of the data. Instead, the covariance matrices used by the algorithm were determined as follows. Two sets of frequency estimates were obtained by curve-fitting the same frequency response functions using two different modal parameter estimators. The first set are the frequencies obtained via Polyreference<sup>18</sup> and given in Table 3, while the second set was obtained using a time and frequency domain procedure<sup>19</sup>. Assuming the experimental frequency errors were normally distributed across the modes, a variance for the distribution,  $\sigma_{\omega}^2$ , was estimated from the differences between the frequency sets. This variance was estimated to be  $\sigma_{\omega}^2 = 0.1140(\text{rad/s})^2$ . The covariance matrix  $Q_{\omega^2}$  is then given as

$$Q_{\omega^2} = 4\sigma_{\omega}^2\Omega^2 + 2(\sigma_{\omega}^2)^2 I \quad (37)$$

where  $\Omega^2 = \text{diag}(\omega_{Ei}^2)$  is the diagonal matrix of the test eigenvalues.

The covariance matrix for the experimental mode shapes was obtained by assuming an expected value for the MAC<sup>14</sup> and relating that to an assumed error normally distributed across the elements of the mode shape vector. Given this assumption, the covariance matrix for  $\phi_{mi}$  is<sup>20</sup>

$$Q_{\phi_{mi}} = \left( \frac{(1 - E[MAC_i])\phi_{mi}^T\phi_{mi}}{N_m - 1} \right) I \quad (38)$$

For the present analysis, the expectation for the MAC was assumed as  $E[MAC_i] = 0.9990$  for all modes. The physical interpretation of this procedure is as follows: assume a series of modal tests on the same structure were performed, each leading to an estimate of the mode shapes with respect to the same set of measurement points. From this series of tests, a mean value for each of the mode shape vectors can be obtained. Then the MAC can be computed between each test mode shape and the mean mode shape from the

series of tests. The parameter  $E[MAC]$  in Eqn. (38) is the mean of the computed MACs across the series of tests. Specifically, for  $k$  tests,

$$E[MAC_i] = \frac{1}{k} \sum_{j=1}^k \frac{|\phi_i^{(j)T} \bar{\phi}_i|^2}{(\phi_i^{(j)T} \phi_i^{(j)})(\bar{\phi}_i^T \bar{\phi}_i)}, \quad \phi_i = \frac{1}{k} \sum_{j=1}^k \phi_i^{(j)} \quad (39)$$

Thus  $E[MAC_i]$  is an expression of the uncertainty or error between different estimates of the same set of modal vectors, and by assuming a normal distribution of errors across the measurement points, is related to the covariance matrix by Eqn. (38).

The initial variances of the parameters were obtained by assuming that the initial joint spring distributions were normal and centered at the initial parameter values with standard deviations equal to 100% of the parameter value. The beam area distributions were assumed to have standard deviations of 3% of their initial values. All initial covariances between the parameters are assumed to be zero, such that the matrix  $Q_p$  is diagonal with the variances of each of the parameters on the diagonal. Assuming a normal distribution for the parameters is not technically correct, since it allows for the possibility of the parameters taking on negative values which is not physically possible. Using normal distributions is simply a convenience which simplifies the Bayesian estimation to the least-squares form of Eqn. (34).

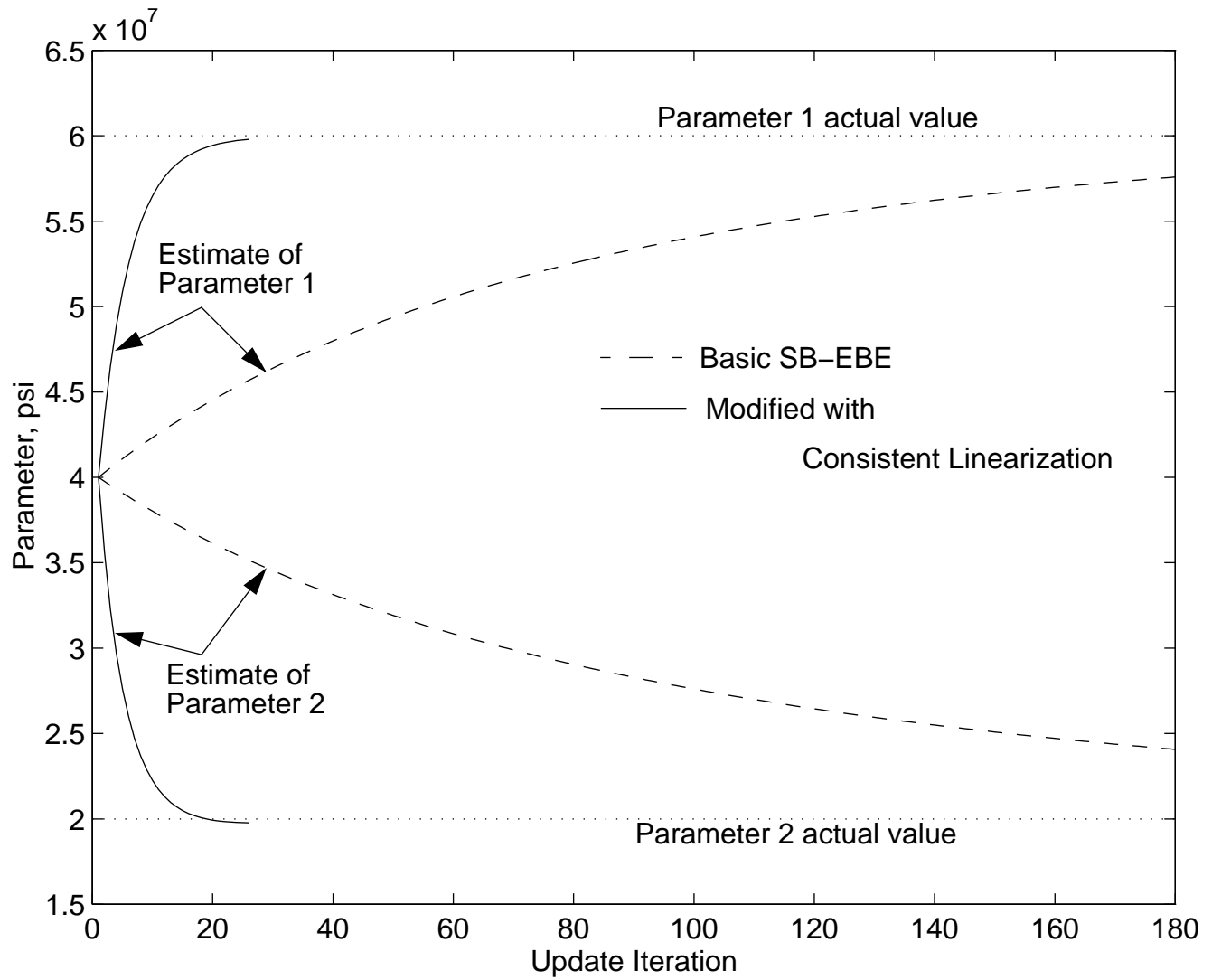


**Figure 1: Convergence of Parameters for Numerical Example**

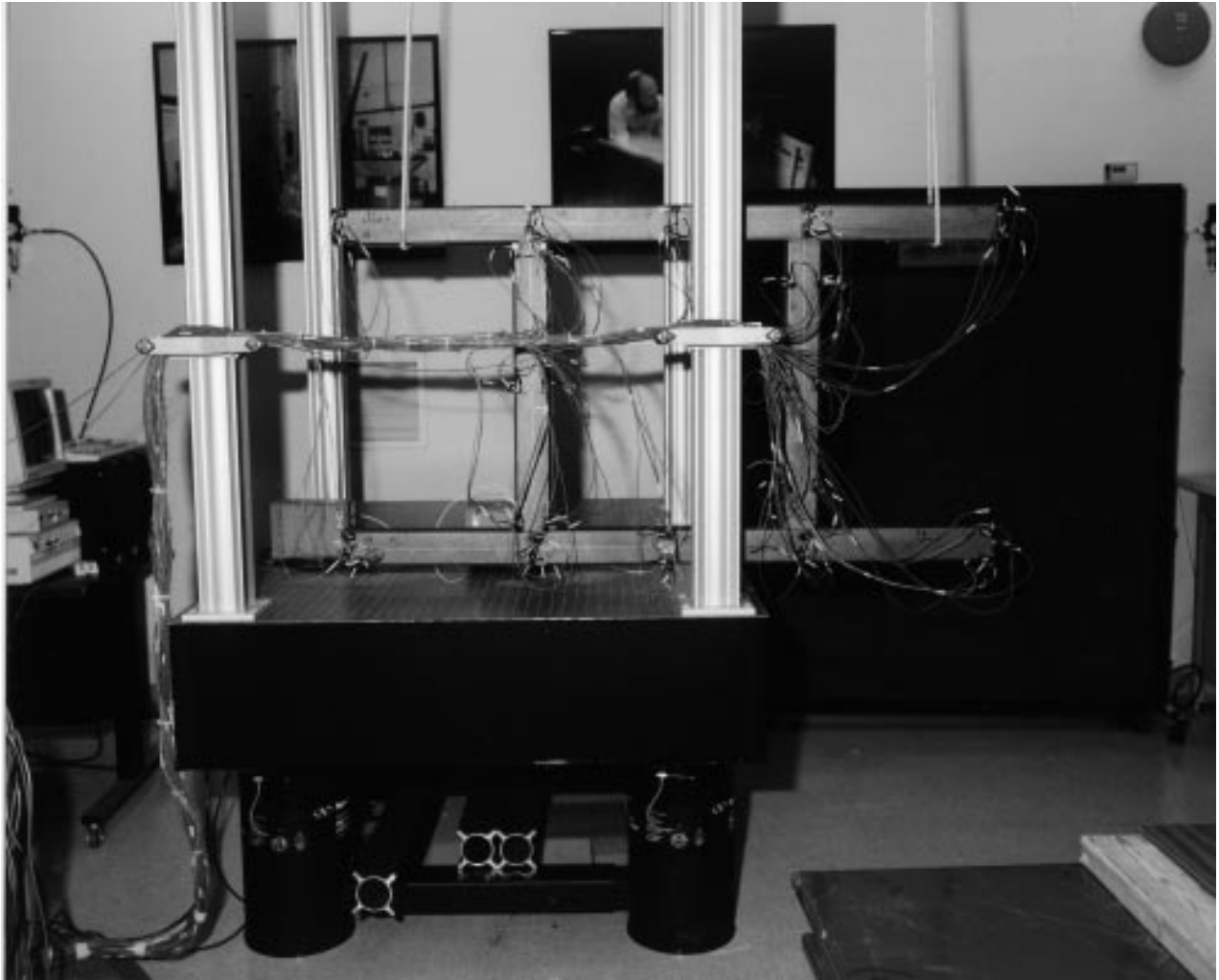


**Figure 2: Modal Testing Setup for LADDER Structure**

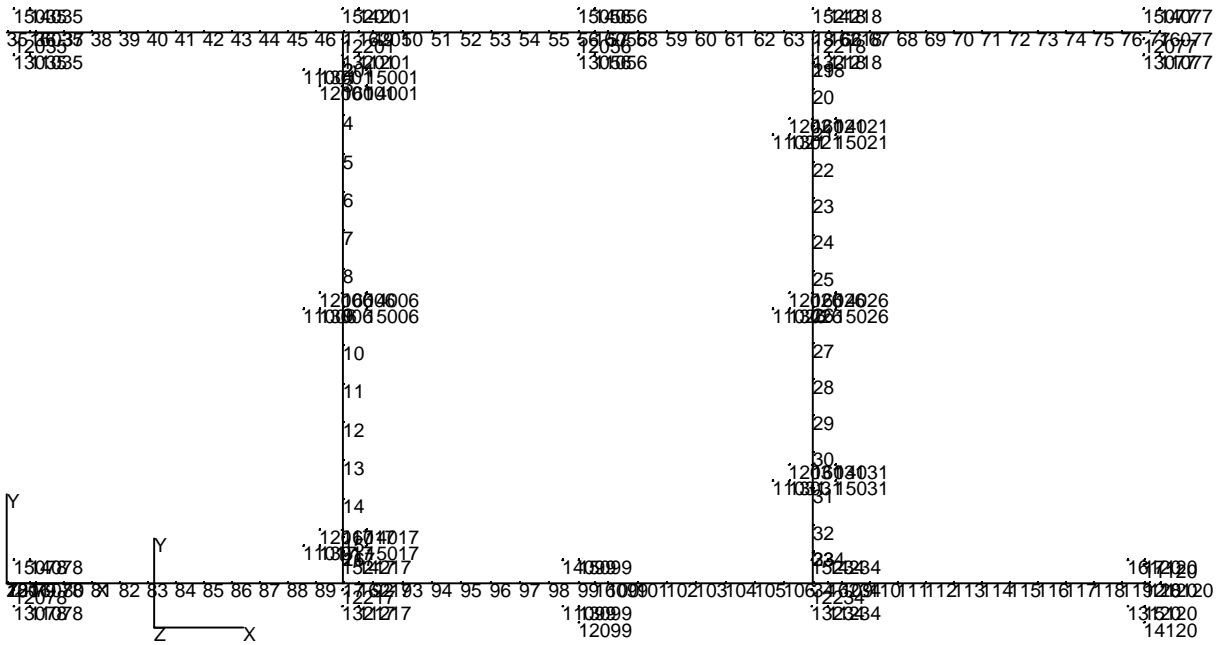


**Figure 3: Finite Element Model of LADDER Structure**

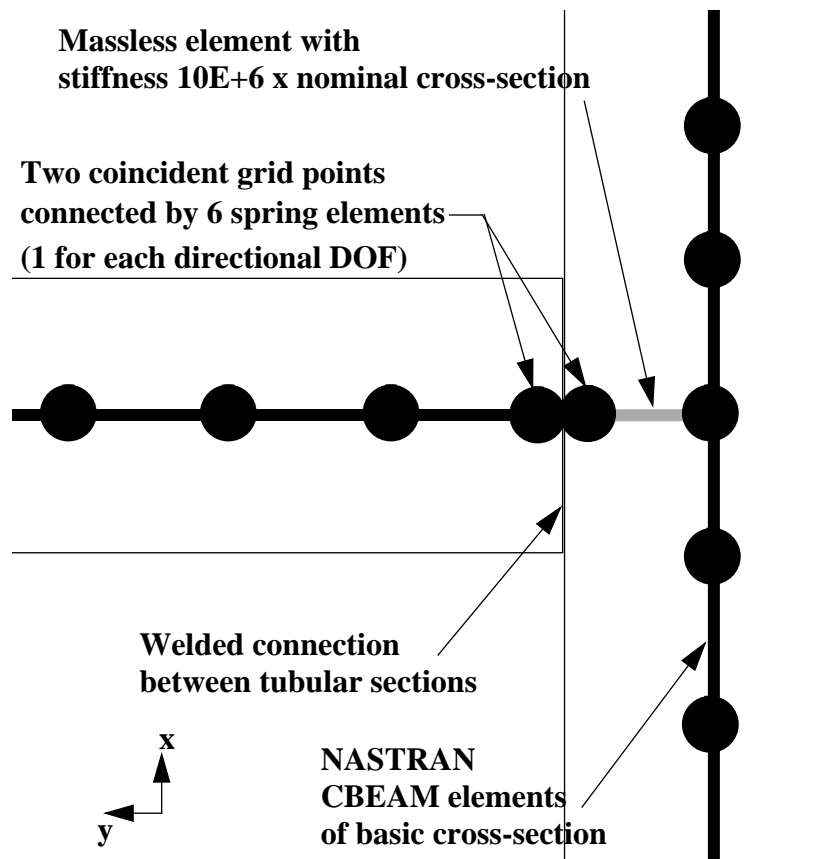


**Figure 4: Modeling Detail for Welded Joint**

## LIST OF FIGURES

Figure 1: Convergence of Parameters for Numerical Example

Figure 2: Modal Testing Setup for LADDER Structure

Figure 3: Finite Element Model of LADDER Structure

Figure 4: Modeling Detail for Welded Joint

